Laser and Particle Beams (2002), *20*, 255–261. Printed in the USA.

DOI: 10.1017/S0263034602202153

Modeling of supersonic jet formation in conical wire array *Z*-pinches

A. CIARDI, S.V. LEBEDEV, J.P. CHITTENDEN, AND S.N. BLAND
The Blackett Laboratory, Imperial College, London SW7 2BZ, UK

(RECEIVED 13 November 2001; ACCEPTED 9 December 2001)

Abstract

Supersonic jet production in conical wire array *Z*-pinches is modeled using a two-dimensional (2D) resistive magneto-hydrodynamic (MHD) code. In conical wire arrays, the converging plasma ablated from the wires stagnates on axis, forming a standing conical shock which redirects and collimates the flow into a jet. As the jet exits the collimator shock, it is radiatively cooled and accelerated by the steep thermal gradients present. Purely hydrodynamic simulations using conditions relevant to the MAGPIE facility show good agreement with the experiments (Lebedev *et al.*, 2002), indicating that narrow, high Mach number ($M \sim 20$), radiatively cooled tungsten jets of astrophysical relevance can be obtained. To investigate the effects of lower radiative cooling on jet collimation, we modeled an aluminum conical wire array. When radiative losses are less significant, lower Mach number ($M \sim 10$), less collimated jets are obtained. MHD simulations relevant to the "Z" facility were carried out to investigate the scaling of jet parameters. The resulting hypersonic ($M \sim 40$), high density jets should allow the investigation of a wider range of astrophysical jet conditions.

Keywords: Jets and outflows; Laboratory astrophysics; Wire array *Z*-pinches

1. INTRODUCTION

Many astrophysical objects have highly collimated outflows (jets) associated with them. They are found in a variety of environments: in active galactic nuclei (AGN; Leahy, 1991), in young stellar objects (YSOs; Mundt *et al.*, 1987; Reipurth *et al.*, 1997), and in planetary nebulae (PNs; Soker & Livio, 1994; Sahai, 2000). These flows are generally characterized by high Mach numbers ($M \geq 10$), and they are well collimated and narrow, with length-to-width ratios that can be 100 or more in Herbig–Haro jets, which are launched by newly formed stars (Reipurth *et al.*, 1996). Although the collimation of these jets is not completely understood, numerical calculations suggest that radiative cooling may play a fundamental role (Blondin *et al.*, 1990; Stone & Norman, 1993; Mellema & Frank, 1997). Other examples of unresolved issues are the dynamical effects of the magnetic fields, the role played by instabilities in jet-ambient interactions, and the nature and evolution of the high density knots observed along the jet beam. In this context, the ability of carrying out scaled experiments is highly desirable.

Address correspondence and reprint requests to: A. Ciardi, Plasma Physics Group, Blackett Laboratory, Imperial College, London SW7 2BZ, U.K. E-mail: a.ciardi@ic.ac.uk

The goal of laboratory astrophysics is to reproduce in a controlled laboratory environment conditions and processes which may be scaled to the astrophysical context, thus providing a further testbed for both theory and numerical models. Similarity criteria between the equations governing the astrophysical and the laboratory processes were discussed by Ryutov *et al.* (1999, 2001), both in the hydrodynamic and magneto-hydrodynamic regimes. In the past few years, a number of scaled experiments have been conducted using intense lasers. These studies may help to shed some light on a variety of issues: core collapse and remnants in supernovae, gamma-ray burst, and planetary interiors (see Remington *et al.*, 2000, for a review). Recent work has also shown the feasibility of producing radiative jets of astrophysical relevance (Farley *et al.*, 1999; Shigemori *et al.*, 2000; Stone *et al.*, 2000).

A novel approach in generating radiatively cooled jets is by imploding conical wire arrays using a *Z*-pinch machine (Lebedev *et al.*, 2002). In these experiments, it was shown, for example, that the importance of radiative cooling on the jet evolution and therefore its dynamical properties can be adjusted by an appropriate choice of wire material. In this article we present the results from the computational modeling of the jets produced using conical wire arrays. The

article is organized as follows. In Section 2, we describe the experimental setup and the formation and launching of jets in *Z*-pinches. The model employed in the simulations and the initial conditions are described in Section 3. Section 4 deals with the results of the simulations, and in Section 5, we present our conclusions and discuss these results and the possibility of scaling the experiments to the astrophysical environment.

2. JET FORMATION IN CONICAL WIRE ARRAYS

The schematic of the experimental configuration is shown in Figure 1a. The load, consisting of a conical array of thin metallic wires, was electro-magnetically driven on the MAGPIE pulsed power facility at Imperial College (Mitchell *et al.*, 1996). A review of *Z*-pinch machines and the physics involved can be found in Ryutov *et al*. (2000).

A peak current of 1 MA with a 240-ns rise time is applied to the conical wire array. Within a few nanoseconds of the start of the current pulse, the wires are converted by resistive heating into a heterogeneous structure consisting of a cold dense core surrounded by a hot (∼25 eV) low density ($n_e \sim 10^{17}$ cm^{-3}, where n_e is the electron density) coronal plasma (Lebedev *et al.*, 1999). The net $\mathbf{J} \times \mathbf{B}$ force, generated by the global magnetic field, accelerates the plasma towards the axis, and the persistence of the wires' core during the current pulse produces a continuous (∼200 ns) converging plasma flow with a velocity $v_{streams} \sim 1.5 \cdot 10^5$ m s^{-1} and a corresponding Mach number $M \sim 5$ (Lebedev *et al.*, 1999). Because of the current pulse short rise time, the majority of the current flows in the path with the smallest inductance at the largest radius, thus remaining in the proximity of the wire cores. Based on 2D MHD simulations in the r–θ plane it appears that little magnetic field is present in the stagnated plasma or in the jets produced (Chittenden *et al.*, 1999). Whether this field is dynamically important is one of the issues that are currently being investigated.

The supersonic coronal plasma streams converge on the axis forming a standing conical shock, which redirects and collimates the flow in the axial direction. The flow then exits the collimator shock and a jet is launched into the region above the anode plate. Figure 1b shows the soft X-ray self-emission at 195 ns from the conical shock produced in an aluminum conical wire array. While the kinetic energy associated with the radial velocity of the flow is thermalized and radiated away, the axial momentum is conserved by the jet. Figure 1c shows a Schlieren image of a tungsten jet at 313 ns (see Lebedev *et al.*, 2002).

In astrophysics, the hydrodynamic mechanism of jet formation through the convergence of conical flows was investigated by Canto *et al.* (1988) in the context of jet production in YSOs. They showed that narrow, well-collimated jets can be produced by a standing conical shock. Further work relevant to YSO and PNs on the mechanism by which conical shocks can arise naturally in stellar wind blown bubbles was articulated by Frank *et al.* (1996). Recently, observations of what appears to be an asymmetric stellar wind collimated into jets by a pair of conical shocks in a proto-PN were reported by Borkowski and Harrington (2001).

3. THE MODEL

The model used is based on the 2D (r, z) resistive magneto-hydrodynamic (MHD) code described by Chittenden *et al.* (1997) and Bell (1994). Explicit hydrodynamics is performed on an Eulerian grid using second order Van Leer advection (as interpreted by Youngs, 1982). Reflective

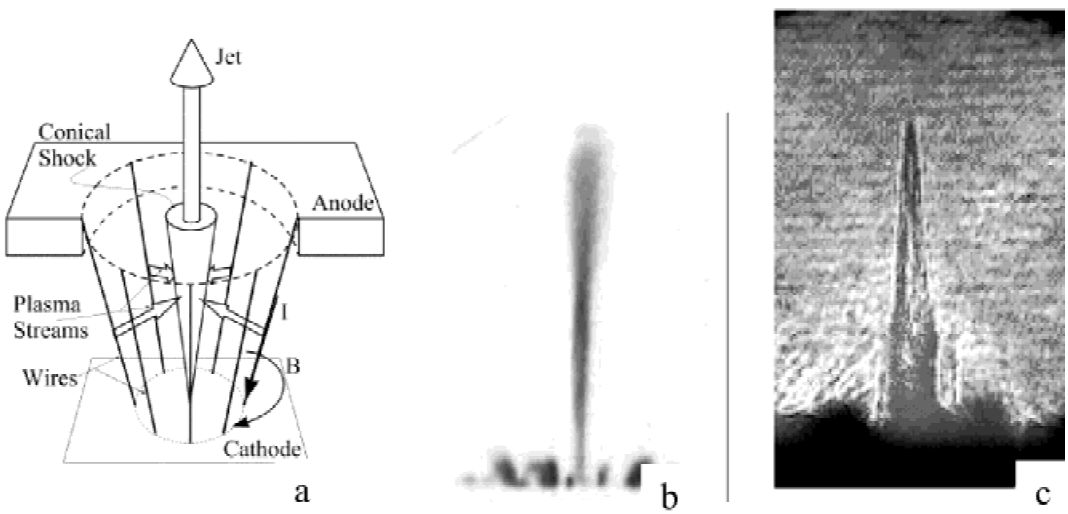

Fig. 1. a: Schematic of the experiment; the global magnetic field **B** and the current *I* are also shown. b: Soft X-ray self-emission from the conical shock produced by an aluminum conical wire array on MAGPIE at 195 ns. The 1.5-μm polycarbonate filter used provided a transmission window between 180 and 290 eV. c: Laser probing image of a tungsten jet on MAGPIE at 313 ns showing propagation of the jet above the anode plate.

https://doi.org/10.1017/S0263034602202153 Published online by Cambridge University Press

boundaries conditions are used at the axis of symmetry, with free-flow conditions at the other boundaries. The thermal and magnetic-field diffusion are backward differenced and solved implicitly by quin-diagonal matrix solution using the ICCG iterative method of Kershaw (1978). The model is two temperature with the ion and electron energy equations coupled by an equilibration term. The different ionization stages are calculated assuming local thermodynamic equilibrium (LTE). Radiative effects are modeled by simple optically thin recombination radiation losses modified to include a probability of escape, allowing a smooth transition to black-body emission in the dense regions. Material with a density below 10^{-4} kg m^{-3} is identified as vacuum, and it is given an artificially high resistivity and thermal conductivity, ensuring that it is isothermal and current free.

In the very early stages of the current pulse, the interaction on axis of the ablated plasma cannot be correctly described by the fluid and LTE assumptions. The density of the converging plasma is too low, and the mean free path of the ions is large compared to the typical scale length of the system (e.g., the size of the precursor plasma). However, the rapid increase in density in the plasma streams and therefore of the plasma on axis insures that within a short time, compared to the time scale of the process, the density increases considerably and the plasma becomes highly collisional. Thus the LTE and fluid assumptions become valid and the model described can be correctly employed.

Two types of simulations were carried out: MHD and purely hydrodynamic (i.e., with the magnetic field turned off). Injection of coronal plasma onto the computational grid was implemented according to a phenomenological model of ablation rate presented by Lebedev *et al.* (2001). This model takes into account the experimental evidence that only a fraction of the mass of the wires is ablated and accelerated towards the axis during the current pulse. We stress here that in cylindrical wire arrays, the load is designed so that the wires run out of mass at about the peak current, and the magnetic field then implodes the whole array. In the jet experiments with conical arrays, we want to maximize the time of plasma injection; therefore the array is "overmassed" such that the wires do not run out of mass during the current pulse and the array does not fully implode. For a conical array, the mass ablation rate per unit length at a position x along the wire (with $x = 0$ at the base of the wire) is given by (see Section III in Lebedev *et al.*, 2001)

$$\frac{dm}{dt} = \frac{10^{-7}(I(t))^2}{(R_0 + x\sin(\theta))\cdot v_{streams}}, \tag{1}$$

where θ is the angle between the wires and the z-axis, $I(t)$ is the current, and R_0 is the smaller radius of the array. Injection of the plasma through the boundary, onto the computational grid, was implemented using Eq. (1) with $v_{streams} = 1.5\cdot10^5$ m s^{-1} and a current waveform relevant to the MAGPIE generator. The hydrodynamic simulations were carried out on a grid with 80 radial and 300 axial cells with a 100-μm resolution (an example, discussed later, is shown in Fig. 2). Injection of plasma at the outer radial boundary was also timed, from the start of the current pulse, to mimic the arrival of plasma from the wires (which are completely outside the computational grid) to the boundary. The conical arrays used in the experiments and considered in the simulations presented in this article are composed of 16 wires inclined at an angle $\theta = 30°$ with respect to the z-axis. The height and the smaller diameter of the array are 10 mm and $R_0 = 8$ mm respectively; the diameter of the wires is 25 μm for aluminum and 18 μm for tungsten.

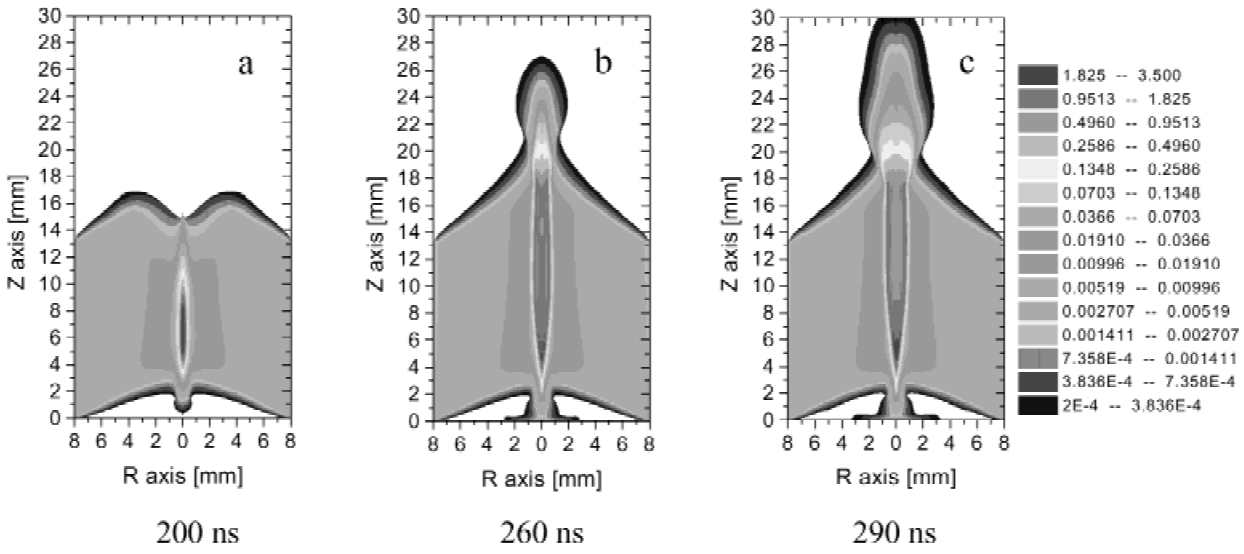

Fig. 2. A series of logarithmic mass density contour maps from a 2D (r, z) hydrodynamic simulation of a tungsten conical wire array on MAGPIE.

https://doi.org/10.1017/S0263034602202153 Published online by Cambridge University Press

We also present here some preliminary MHD simulations results relevant to the "Z" facility at Sandia National Laboratories (peak current ~ 20 MA with a 120-ns rise time) for a conical array composed of 120 tungsten wires with a 30.5-μm diameter; the smaller radius of the array is 10 mm and the wires are inclined at an angle $\theta = 30°$. In the MHD simulations, (Fig. 3) material was sourced on the computational grid according to Eq. (1) with $v_{streams} = 2.5 \cdot 10^5$ m s^{-1}, which is consistent with the experimental observation of precursor plasma on axis (Cuneo *et al.*, 2001). The magnetic field was set at outer radial boundary using an experimental current waveform. (Cuneo *et al.*, 2001). Because of the more demanding computational time requirements, due to the inclusion of the magnetic field, a lower resolution of 200 μm on a grid of 100 × 150 cells was employed. Although such a low resolution underresolves the important structures in the jet, in particular the conical shock, these simulations are primarily intended to investigate the scaling of the jet parameters to a larger facility.

4. SIMULATIONS RESULTS

The time evolution of a tungsten jet is shown in Figure 2. At 200 ns (Fig. 2a), a dense plasma has already stagnated on axis and a standing shock begins to form. As the converging plasma crosses the shock, the kinetic energy associated with its radial momentum is thermalized, while the axial momentum (tangential to the shock) is conserved in the compressed flow. The flow is then redirected and collimated into a jet by the now well-developed conical shock (Fig. 2b,c). Ionization also occurs across the shock; the average ionic charge is $Z^* \sim 10$ in the plasma streams and $Z^* \sim 22$ in the conical shock. As the jet leaves the formation region ($z \sim 18$ mm) and propagates into the vacuum, it expands due to its large "overpressure." A freely expanding supersonic jet diverges at an angle given by

$$\phi = 2 \tan^{-1}\left(\frac{1}{M}\right), \tag{2}$$

where M is the local Mach number of the flow. For a tungsten jet, $M \sim 20$, giving a divergence angle $\phi \sim 6°$. Figure 4a shows, for the same simulation, the axial profiles of temperature and density averaged over the first five radial cells at 290 ns. The jet formation region extends from ~5 mm to ~18 mm. Within this region, the small negative axial gradients are a direct consequence of the different mass ablation rates along the wires and, therefore, of the axial variation of plasma density just upstream of the shock. In particular, the shock strength (defined as the ratio of the downstream density to the upstream density) is constant along the length of the conical shock (~40), with small variations being produced by both the varying opening angle of the conical shock, which determines the upstream shock velocity, and by the postshock equilibrium temperature (Canto *et al.*, 1988). As the flow exits the collimator shock it expands, leading to rarefaction and cooling of the plasma. The cooling length (the distance over which the temperature drops to some lower equilibrium value) is $l_c \sim 2$–3 mm. Expansion alone is not sufficient to produce such a short cooling length; in fact, simulations where the radiative losses were switched off suggest a cooling length of at least ~12 mm. Therefore, cooling of the jet is dominated by radiative losses, at least in high Z elements. As the jet rapidly radiates away its thermal energy, a steep negative pressure gradient is set up which acts to accelerate the jet over a length ~l_c, with the accel-

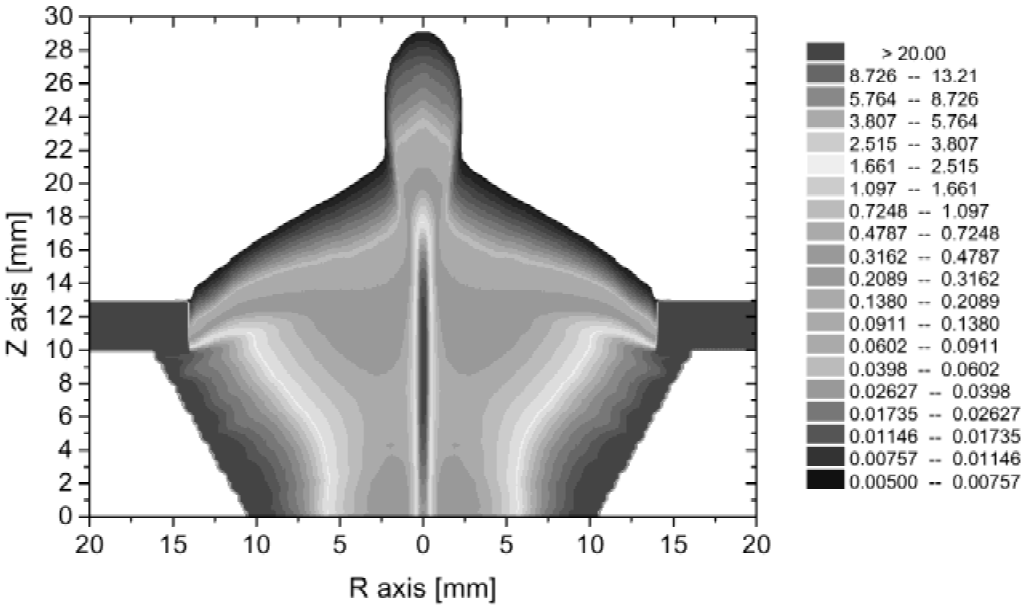

Fig. 3. Logarithmic mass density contour map at 170 ns from a 2D (r, z) MHD simulation of a tungsten conical wire array on "Z."

https://doi.org/10.1017/S0263034602202153 Published online by Cambridge University Press

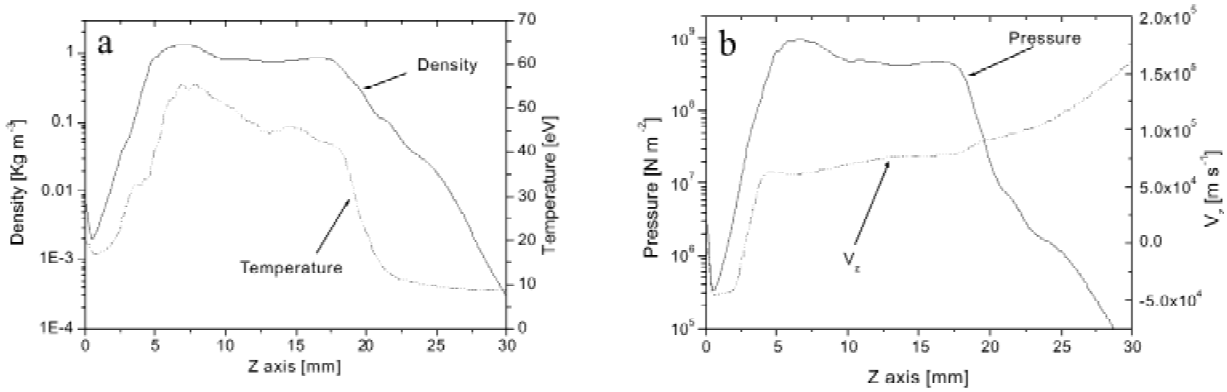

Fig. 4. Axial profiles at 290 ns, averaged over the first five radial cells, from a 2D (r, z) simulation of a tungsten conical wire array on MAGPIE. a: Density (——) and temperature (------). b: Pressure (——) and axial velocity V_z (------).

eration being more efficient the lower the density. Therefore, because the density of launched jet material increases with time, the axial velocity v_z increases along the jet axis (Fig. 4b). Also along the jet ($z \geq 20$ mm), both the temperature and the effective charge ($Z^* \sim 12$) are constant, indicating that the Mach number is also increasing, thus leading to a differential expansion of the jet. The head of the jet ($M \sim 20$), formed earlier in time when the opening angle of the conical shock was small, will therefore maintain its shape almost unchanged, while the jet beam near the base ($M \sim 6$) will expand considerably more and from a larger initial size. This apparent negative angle of convergence at the jet tip was observed experimentally in tungsten jets by Lebedev *et al.* (2002; also see Fig. 1c); an estimate of the Mach number was also given in the range $M \sim 20$.

To investigate the role played by radiative losses on the dynamics of jet formation and propagation, we have carried out a series of simulations for a lower Z element, namely aluminum. A typical jet produced is shown in Figure 5. The hydrodynamic process of jet formation is similar to that of a tungsten wire array, and here we show the aluminum jet at 240 ns, when its propagation length is about equal to that of a tungsten jet at 260 ns. To take into account the experimental evidence that in aluminum wire arrays a precursor is visible about 20–30 ns earlier than in tungsten wire arrays (Lebedev *et al.*, 1999), a time lag between the two simulations was introduced by delaying the injection of plasma at the radial outer boundary. The simulations show that for a low Z element, a significantly less collimated and wider jet is produced. The diameter at the base of the jet is ~4–5 mm (240 ns) compared to ~2–3 mm (260 ns) of a tungsten jet. The experimental values measured from the X-ray self-emission at the base of the jet are ~3.5 mm and ~2.5 mm for aluminum and tungsten respectively (Lebedev *et al.*, 2002). Density in the conical shock is lower in aluminum, indicating a weaker shock strength of ~17. The ionization of the plasma across the shock goes from $Z^* \sim 5$ in the plasma streams to $Z^* \sim 10$ in the conical shock. The effects of radiative cooling are evident in Figure 6a,b, which show for the same simulation at 240 ns the axial profiles of temperature, density, axial velocity v_z, and pressure averaged over the first five radial cells. Again, the jet is accelerated as it exits the conical shock, but the less efficient radiative cooling means that the temperature drop is less steep than for tungsten, and an effective charge $Z^* \sim 7$ is obtained along the jet. The cooling length, as the temperature drops from ~40 eV to ~25 eV, is $l_c \sim 10$ mm for aluminum, compared to $l_c \sim 2$ mm seen for tungsten. In Lebedev *et al.* (2002), an emission length of ~7 mm for aluminum and ~2 mm for tungsten was observed. The less efficient radiative cooling in aluminum produces a lower Mach number flow than in tungsten. Along the axis ($z \geq 20$ mm) in fact,

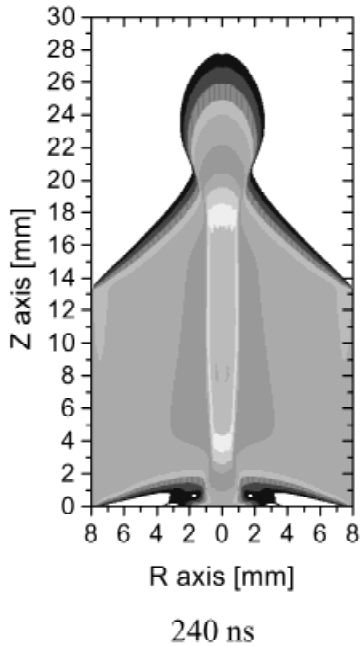

Fig. 5. Logarithmic mass density contour map from a 2D (r, z) hydrodynamic simulation of an aluminum conical wire array on MAGPIE (contours as in Fig. 2).

https://doi.org/10.1017/S0263034602202153 Published online by Cambridge University Press

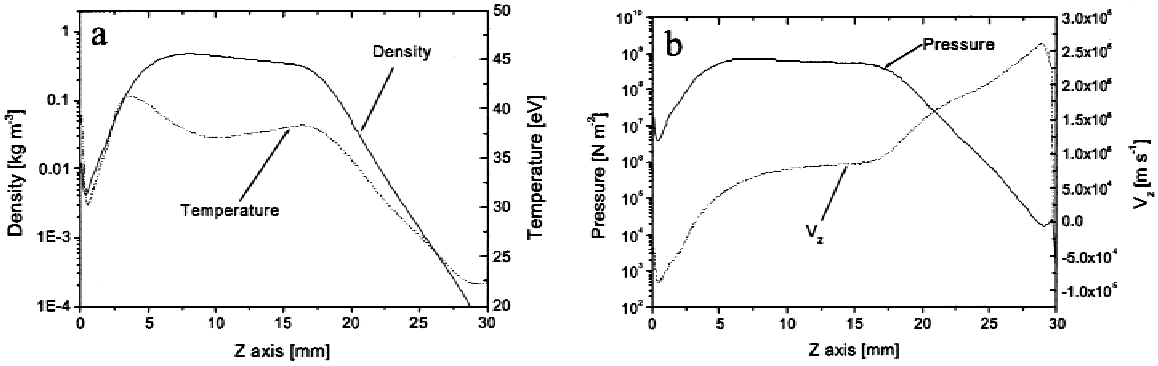

Fig. 6. Axial profiles at 220 ns, averaged over the first five radial cells, from a 2D (r, z) simulation of an aluminum conical wire array on MAGPIE. a: Density (——) and temperature (------). b: Pressure (——) and axial velocity V_z (------).

the Mach number for an aluminum jet varies from $M \sim 2$ to $M \sim 10$, leading on average to a larger divergence angle.

To investigate how the jets would scale to a larger facility, we have run a series of low resolution MHD simulations relevant to the "Z" generator. The evolution of the jet is qualitatively similar to that shown in the hydrodynamic simulations. A comparison between some of the jet's parameters obtained for MAGPIE and "Z" conditions are shown in Table 1. While the length and size of the jets are comparable for the two facilities, higher velocities $v_{jet} \sim 5 \cdot 10^5$ m s^{-1} and higher densities $\rho_{jet} \sim 10$ kg m^{-3} are expected for the jets on "Z." Radiative cooling is still dynamically dominant, giving rise to hypersonic jets with $M \geq 40$ and a kinetic energy of ~100 kJ.

5. CONCLUSIONS

We presented a series of simulations of jets produced by the implosion of conical wire arrays on the MAGPIE generator. The results, which reproduce the experiments well, show that collimated, high velocity $v_{jet} \sim 2 \cdot 10^5$ m s^{-1}, high Mach number jets ($M \sim 20$) are produced by the convergence of conical plasma flows. The standing conical shock formed on axis acts to redirect and collimate the flow into a jet. Furthermore, radiative cooling of the plasma sets up a steep pressure gradient that accelerates the jet as it exits the formation region. It was also shown that the collimation of the jet is strongly dependent on the radiative losses, with high Z elements producing narrow and better collimated jets.

Table 1. *Jet parameters on MAGPIE and "Z"*

Facility (current)	Radius (mm)	Length (mm)	Velocity (m/s)	Density (kg m^{-3})	Kinetic energy (kJ)
MAGPIE (1 MA)	~1	~20	~$2 \cdot 10^5$	~10^{-1}	~0.2
Z (20 MA)	~2	~20	~$5 \cdot 10^5$	~10	~100

The global properties of laboratory and astrophysical jets can be characterized by three dimensionless parameters (Blondin *et al.*, 1990): the Mach number M, the cooling parameter $\chi = l_c/r_{jet}$ (defined as the ratio of the cooling length l_c to the jet radius r_{jet}), and the density contrast $\eta = \rho_{jet}/\rho_{ambient}$ (defined as the ratio of jet to ambient density). Typical values found in astrophysical jets are $M > 10$, $\chi \leq 1$ and $\eta \geq 1$. From the simulation, we conclude that the tungsten jets produced have comparable dimensionless parameters: $M \geq 20$ and $\chi \leq 1$; the density contrast in these experiments is not defined since the jet is propagating in vacuum. In particular, η can be "adjusted" in the experiments by introducing a target plasma. Preliminary jet–target interactions have been carried out by Lebedev *et al.* (2002) using side and end-on thin-foil solid targets. In the experiments, the jet was observed to interact with the radiatively ablated plasma from the targets in what actually appears to be a collisionless interaction, at least with the side-target configuration where the jet is seen to bend. Scaling to a larger facility like "Z" would allow the investigation of hypersonic jet–target interaction for a wider range of density contrast. Furthermore, the higher densities obtained in the jet should result in jet–target interactions in the collisional regime. A second set of dimensionless parameters, which need to be taken into consideration when scaling to astrophysics, regard the role of dissipative processes in the plasma and its departure from an ideal fluid. These parameters are considered in detail in Lebedev *et al.* (2002), where it is shown that their values are within the correct regime for the scaling requirements.

Although the hydrodynamic simulations reproduce the gross behavior of the jets, further work with high-resolution MHD simulations is needed to investigate in detail the effects of the magnetic field on the jet formation and propagation. These will also provide a framework for fully 3D simulations of jets, which are currently limited to low resolution by the prohibitive computational times involved.

https://doi.org/10.1017/S0263034602202153 Published online by Cambridge University Press

ACKNOWLEDGMENTS

The authors thank Dr. Adam Frank and Dr. Eric Blackman of the University of Rochester for useful discussions on the relevance of these experiments to astrophysical jets. We also thank Dr. Chris Deeney of Sandia National Laboratories for useful discussions on the extension of these experiments to larger scale facilities.

REFERENCES

Bell, A.R. (1994). Magnetohydrodynamic jets. *Phys. Plasmas* **1**, 1643–1652.

Blondin, J.M., Fryxell, B.A. & Königl, A. (1990). The structure and evolution of radiatively cooling jets. *Astrophys. J.* **360**, 370–386.

Borkowsky, K.J. & Harrington, J.P. (2001). Kinematics of 1200 kilometer per second jets in He 3-1475. *Astrophys. J.* **550**, 778–784.

Cantó, J. Tenorio-Tagle, G. & Rózyczka, M. (1988). The formation of interstellar jets by the convergence of supersonic conical flows. *Astron. Astrophys.* **192**, 287–294.

Chittenden, J.P., Aliaga-Rossel, R., Lebedev, S.V., Mitchell, I.H., Tatarakis, M., Bell, A.R. & Haines, M.G. (1997). Two-dimensional magneto-hydrodynamic modeling of carbon fiber *Z*-pinch experiments. *Phys. Plasmas* **4**, 4309–4317.

Chittenden, J.P., Lebedev, S.V., Bell, A.R., Aliaga-Rossel, R., Bland, S.N. & Haines, M.G. (1999). Plasma formation and implosion structure in wire array *Z* pinches. *Phys. Rev. Lett.* **83**, 100–103.

Cuneo, M.E., Chandler, G.A., Vessey, R.A., Porter, J.L., Nash, T.J., Bailey, J.E., Aragon, R.A., Fowler, W.E., Stygar, W.A., Struve, K.W., Torres, J.A., McGurn, J.S., Lazier, S.E., Nielson, D.S., Chittenden, J.P. & Lebedev, S.V. (2001). *Bull. Am. Phys. Soc.* **46**, 234.

Farley, D.R., Estabrook, K.G., Glendinning, S.G., Glenzer, S.H., Remington, B.A., Shigemori, K., Stone, J.M., Wallace, R.J., Zimmerman, G.B. & Harte, J.A. (1999). Radiative jet experiments of astrophysical interest using intense lasers. *Phys. Rev. Lett.* **83**, 1982–1985.

Frank, A., Balick, B. & Livio, M. (1996). A mechanism for the production of jets and ansae in planetary nebulae. *Astrophys. J.* **471**, L53.

Kershaw, D.S. (1978). *J. Comput. Phys.* **26**, 43.

Leahy, J.P. (1991). In *Beams and Jets in Astrophysics* (Hughes, P., Ed.). Cambridge University Press.

Lebedev, S.V., Aliaga-Rossel, R., Bland, S.N., Chittenden, J.P., Dangor, A.E., Haines, M.G. & Mitchell, I.H. (1999). The dynamics of wire array Z-pinch implosions. *Phys. Plasmas* **6**, 2016–2022.

Lebedev, S.V, Beg, F.N., Bland, S.N., Chittenden, J.P., Dangor, A.E., Haines, M.G., Kwek, K.H., Pikuz, S.A. & Shelkovenko, T.A. (2001). Effect of discrete wires on the implosion dynamics of wire array Z pinches. *Phys. Plasmas* **8**, 3734–3747.

Lebedev, S.V, Chittenden, J.P., Beg, F.N., Bland, S.N., Ciardi, A., Ampleford, D., Hughes, S., Haines, M.G., Frank, A., Blackman, E.G. & Gardiner, T. (2002). Laboratory astrophysics and collimated stellar outflows: The production of radiatively cooled hypersonic plasma jets. *Astrophys. J.* **564**, 113–119.

Mellema, G. & Frank, A. (1997). Outflow collimation in young stellar objects. *Mon. Not. R. Astron. Soc.* **292**, 795–807.

Mitchell, I.H., Bayley, J.M., Chittenden, J.P., Worley, J.F., Dangor, A.E. & Haines, M.G. (1996). A high impedance mega-ampere generator for fiber *z*-pinch experiments. *Rev. Sci. Instrum.* **67**, 1533–1541.

Mundt, R., Brugel, E.W. & Bührke, T. (1987). Jets from young stars: CCD imaging, long slit spectroscopy, and interpretation of existing data. *Astrophys. J.* **319**, 275–303.

Reipurth, B. (1997). Herbig–Haro Flows and the Birth Low Mass Stars. (Reipurth, B. & Bertout, C., Eds.) *IAU Symposium* No. 182. Dordrecht: Kluwer.

Reipurth, B., Raga, A.C. & Heathcote, S. (1996). HH 110: The grazing collision of a Herbig-Haro flow with a molecular cloud core. *Astron. Astrophys.* **311**, 989–996.

Remington, B.A., Drake, R.P., Takabe, H. & Arnett, D. (2000). A review of astrophysics experiments on intense lasers. *Phys. Plasmas* **7**, 1641–1652.

Ryutov, D.D., Derzon, M.S. & Matzen, M.K. (2000). The physics of fast *Z* pinches. *Rev. Mod. Phys.* **72**, 167–223.

Ryutov, D., Drake, R.P., Kane, J., Liang, E., Remington, B.A. & Wood-Vasey, W.M. (1999). Similarity criteria for the laboratory simulation of supernova hydrodynamics. *Astrophys. J.* **518**, 821–832.

Ryutov, D., Remington, B.A., Robey, H.F. & Drake, R.P. (2001). Magnetohydrodynamic scaling: From astrophysics to the laboratory. *Phys. Plasmas* **8**, 1804–1816.

Sahai, R. (2000). Asymmetrical Planetary Nebulae II. (Kastner, J.H., Soker, N. & Rappaport, S., Eds.) *ASP Conf. Ser.* Vol. 199, 209.

Shigemori, K., Kodama, R., Farley, D.R., Koase, T., Estabrook, K.G., Remington, B.A., Ryutov, D.D., Ochi, Y., Azechi, H., Stone, J. & Turner, N. (2000). Experiments on radiative collapse in laser-produced plasmas relevant to astrophysical jets. *Phys. Rev. E* **62**, 8838–8841.

Soker, N. & Livio, M. (1994). Disks and jets in planetary nebulae. *Astrophys. J.* **421**, 219–224.

Stone, J.M. & Norman, M.L. (1993). Numerical simulations of protostellar jets with nonequilibrium cooling. I—Method and two-dimensional results. II—Models of pulsed jets. *Astrophys. J.* **413**, 198–220.

Stone, J.M., Turner, M., Estabrook, K.G., Remington, B.A., Farley, D.R., Glendinning, S.G. & Glenzer, S. (2000). Testing astrophysical radiation hydrodynamics codes with hypervelocity jet experiments on the nova laser. *Astrophys. J. Suppl. S* **127**, 497–502.

Youngs, D.L. (1982). *Numerical Methods for Fluid Dynamics* (Morton, K.W. & Baines, M.J., Eds.). New York: Academic Press.